Journal of Medicinal Chemistry Article

J. Med. Chem. **2010,** *53,* 8679–8687 **8679**
DOI: 10.1021/jm101179e

Identification and Synthesis of Novel Inhibitors of Acetyl-CoA Carboxylase with in Vitro and in Vivo Efficacy on Fat Oxidation

Stefanie Keil,* Marco Müller, Gerhard Zoller, Guido Haschke, Katrin Schroeter, Maike Glien, Sven Ruf, Ingo Focken, Andreas W. Herling, and Dieter Schmoll

Sanofi-Aventis Deutschland GmbH, R&D, Diabetes Division, Industriepark Hoechst, Building G 878, D-65926 Frankfurt am Main, Germany

Received September 10, 2010

Acetyl CoA carboxylase isoforms 1 and 2 (ACC1/2) are key enzymes of fat utilization and their inhibition is considered to improve aspects of the metabolic syndrome. To identify pharmacological inhibitors of ACC1/2, a high throughput screen was performed which resulted in the identification of the lead compound **3** (Gargazanli, G.; Lardenois, P.; Frost, J.; George, P. Patent WO9855474 A1, 1998) as a moderate selective ACC2 inhibitor. Optimization of **3** led to **4m** (Zoller, G.; Schmoll, D.; Mueller, M.; Haschke, G.; Focken, I. Patent WO2010003624 A2, 2010) as a submicromolar dual ACC1/2 inhibitor of the rat and human isoforms. **4m** possessed favorable pharmacokinetic parameters. This compound stimulated fat oxidation in vivo and reduced plasma triglyceride levels in a rodent model after subchronic administration. **4m** is a suitable tool compound for the elucidation of the pharmacological potential of ACC1/2 inhibition.

1. Introduction

Increased ectopic fat accumulation is a risk factor for the development of type 2 diabetes,[1−23,4] indicating that a reduction of ectopic lipids could be beneficial for the treatment of the metabolic syndrome. The inhibition of acetyl CoA carboxylase (ACC[a]) has received special attention for this approach and has been the focus of drug discovery programs for the identification of ACC inhibitors.[5−7] Examples of previously described compounds include **1**[8−10] and **2**[5,11] (Figure 1).

Mammalian ACC catalyzes the formation of malonyl-CoA and exists in two isoforms with distinct subcellular localizations.[6] Although the functions of these isoforms overlap, cytosolic ACC1 is involved predominantly in de novo lipogenesis, whereas mitochondrial ACC2 controls mainly fat oxidation. In particular, the inhibition of ACC2 has been predicted to reduce intracellular fat by the subsequent switch to fat utilization for energy production. However, the suppression of both ACC1 and ACC2 expression using antisense oligonucleotides stimulates fat oxidation in hepatocytes more potently than that of either ACC1 or ACC2 alone.[12] This indicates that isoform unselective inhibition of ACC is more efficacious in stimulating fat oxidation than an ACC2-selective inhibitor. Therefore, we aimed for the identification of an isoform unselective ACC1/2 inhibitor and describe here the identification and optimization of a new series of ACC1/2 inhibitors with favorable pharmacokinetic parameters and in vivo activity.

2. Chemistry

The synthesis of the first target molecules **4a**−**4d** is shown in Scheme 1. Commercially available 3-benzyloxyphenylacetic acid methyl ester was treated with dimethylcarbonate under basic conditions with subsequent reduction of the ester functions with diisobutylaluminiumhydride to obtain the diol **5**. Transacetalisation with 4-aminobutyraldehyde diethylacetal and acidic catalysis yielded the dioxanyl compound **6**, which was then acetylated, and the benzyl protecting group was removed by hydrogenation to obtain compound **7**. The free phenolic function in **7** was alkylated with different alkyl halides or reacted with different alcohols under Mitsunobu type reaction to obtain compounds **4a**−**4d**.

The synthesis of the target molecules **4e**, **4f**, and **4g** is shown in Scheme 2. Commercially available 5-benzyloxy-2-chloropyridine was substituted with 2-phenyl-[1,3]dioxan-5-ol under basic conditions to obtain dioxanyl compound **8**. Opening of the cyclic acetal under acidic conditions yielded the diol compound **10g**. Alkylation of 4-benzyloxyphenol with dimethyl 2-chloromalonate and subsequent reduction of the ester functions yielded the diol compound **10e**. The diols **10e** and **10g** were elaborated to the target molecules **4e**, **4f**, and **4g** in a similar manner according to Scheme 1.

The synthesis of the target molecules **4h**−**4j** and **4n**−**4p** is shown in Scheme 3. Commercially available *N*-[3-(4-hydroxy-phenyl)-propyl]-acetamide or *N*-[3-(4-hydroxy-phenyl)-1-methyl-propyl]-acetamide were reacted with pyridine or pyrimidine halides under conditions of a nucleophilic aromatic

*To whom correspondence should be addressed. Phone: ++49-69-305-80835. Fax: +496930517373. E-mail: stefanie.keil@sanofi-aventis.com.

[a] Abbreviations: ACC, acetyl CoA carboxylase; DEAD, diethylazodicarboxylate; DIAD, diisopropylazodicarboxylate; DIBALH, diisobutylaluminium hydride; DMAP, 4-(dimetylamino)-pyridine; DCM, dichloromethane; DMF, dimethylformamide; HPLC, high pressure liquid chromatography; MW, microwave; NMP, *N*-methylpyrrolidon; PPh3, triphenylphosphine; pTSOH, *para*-toluenesulfonic acid; RP, reverse phase; SAR, structure−activity-relationship; THF, tetrahydrofuran; TOTU, *O*-((ethoxycarbonyl)cyanomethyleneamino)-*N*,*N*,*N*′,*N*′-tetramethyluronium tetrafluoroborate; HTS, high throughput screen.

Published on Web 11/17/2010

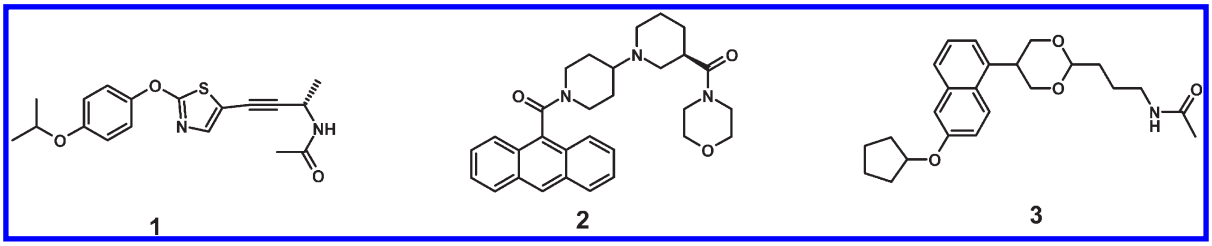

Figure 1. Structures of representative ACC inhibitors from Abbott **1** and Pfizer **2** and of the HTS screening hit **3**.

Scheme 1[a]

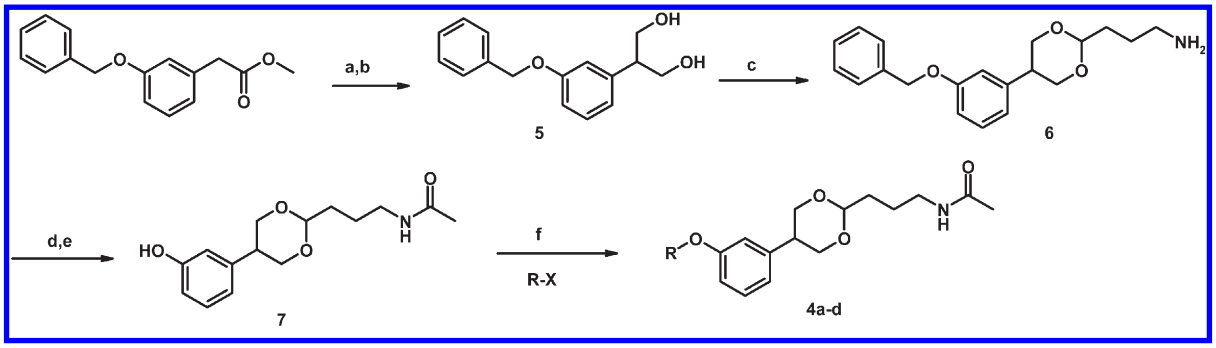

[a] Reagents and conditions: (a) dimethylcarbonate, NaH; (b) DIBALH; (c) 4-aminobutyraldehyde diethylacetal, pTsOH, toluene, 60 °C; (d) Ac_2O, NEt_3, ethyl acetate, RT; (e) H_2 (3 bar)/Pd, ethanol, RT; (f) R-OH, PPh3, DEAD, THF or R-Hal, Cs_2CO_3.

Scheme 2[a]

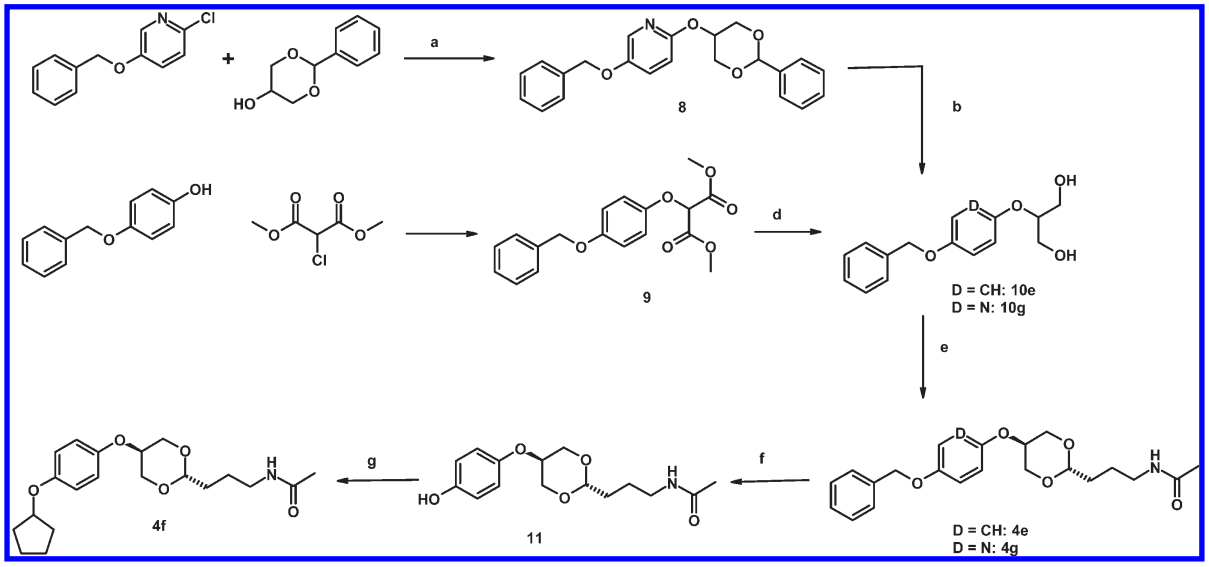

[a] Reagents and conditions: (a) NaH, NMP, MW, 200 °C; (b) HCl, MeOH, RT; (c) Cs_2CO_3, KI, DMF, 60 °C; (d) DIBALH, toluene, 0 °C; (e) *N*-(4,4-diethoxybutyl)acetamide, pTsOH, toluene, 60 °C, separation of isomeres; (f) H_2 (3 bar)/Pd, ethanol, RT; (g) cyclopentylbromide, Cs_2CO_3, DMF, RT.

substitution reaction to obtain target compounds **4h**−**4j** and **4n**−**4p**.

The synthesis of the target molecule **4m** is shown in Scheme 4. Commercially available 6-chloro-pyridin-3-ol and 1,4-dibromobenzene were reacted under copper catalysis at elevated temperature to obtain compound **12**. The chlorine atom was then substituted by isopropoxide. The bromide **13** was then reacted in a Sonogashira reaction with commercially available (*S*)-2-(but-3-yn-2-yl)isoindole-1,3-dione to obtain compound **14**. The triple bond was hydrogenated and the phthalimide protecting group removed by treatment with hydrazine. The free amino function was then acetylated to obtain enantiomeric pure **4m**(ent-*S*).

The synthesis of the target molecules **4q**−**4t** is shown in Scheme 5. Racemic **17** was synthesized in a similar manner according to Scheme 4 by use of racemic 2-(but-3-yn-2-yl)-isoindole-1,3-dione. The amino function of **17** was then further elaborated by known procedures to obtain target molecules **4q**−**4t**.

The synthesis of the target molecules **4u** is shown in Scheme 6. 1,4-*cis*-Cyclohexandiol was reacted with 5-isopropoxy-pyridin-2-ol under Mitsunobu type reaction under inversion of configuration to obtain the 1,4-*trans*-cyclohexandiol derivative **18**. The free hydroxyl group was alkylated with 3-bromo-2-methyl-propene to yield compound **19**. The double bond was bishydroxylated with osmium tetroxid, the diol cleaved with

Scheme 3[a]

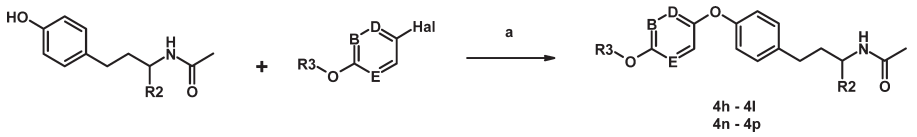

[a] Reagents and conditions: (a) NaH, NMP, MW, 220 °C.

Scheme 4[a]

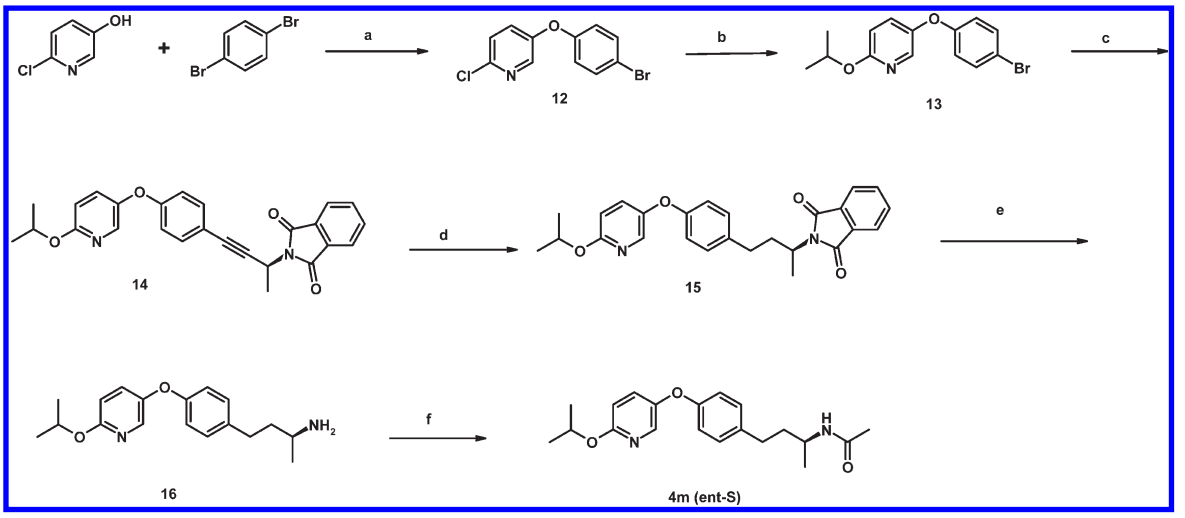

[a] Reagents and conditions: (a) CuO/K_2CO_3, pyridine, 150 °C; (b) isopropyl alcohol, NaH, NMP, 120 °C; (c) 2-((*S*)-1-methyl-prop-2-ynyl)-isoindole-1,3-dione, PPh_3, DEAD, THF; (d) H_2/Pd, EtOH; (e) hydrazine hydrate; (f) Ac_2O, NEt_3.

Scheme 5[a]

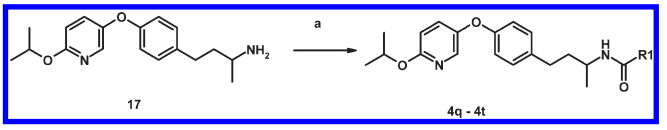

[a] Reagents and conditions: (a) **4q**, 1,1′-carbonyldiimazole, NEt_3, formic acid; **4r**−**4s**, R1COCl; **4t**, **17** was used instead of **16**, NH_3, carbonyldiimidazole, NEt_3.

sodium periodate and the resulting hydroxyl function elaborated to an acetamide function by known procedures to obtain target molecule **4u**, which was separated into its enantiomers on chiral phase.

The synthesis of the target molecules **4v** is shown in Scheme 7. The aromatic ring of commercially available *N*-[(3-(4-hydroxyphenyl)-1-methylpropyl]-acetamide was hydrogenated at high pressure (110 bar) with a rhodium catalyst to obtain the cyclohexyl compound **20**. The free hydroxyl group of **20** was reacted with 2-isopropoxy-5-(4,4,5,5-tetramethyl-1,3,2-dioxaborolan-2-yl)pyridine under copper catalysis to obtain target compound **4v**, which was separated into its isomers on chiral phase.

3. Results and Discussion

3.1. Discovery and Optimization Strategy. Here we report the identification, structure−activity relationship, and lead optimization of novel dioxane derivatives resulting in potent dual ACC1/2 inhibitors. Compound **3** (Figure 1) was discovered from high-throughput screening of our internal compound collection and served as a starting point for optimization. This compound shows an IC_{50} value of 630 nM for human ACC2 (hACC2) and was inactive on human ACC1 (hACC1) and rat ACC1/2 (rACC1/2). This isoform selectivity indicates that **3** binds to a site within ACC that is not fully conserved between the isoforms and between the species. The overall sequence identity between hACC1 and hACC2 is approximately 75% except for an extra 114 amino acids in the N-terminus of ACC2.[13] The sequence identitiy of the rat and human orthologs amounts to 97% (isoform 1) and 90% (isoform 2), respectively.

Our optimization strategy had two goals: Improving chemical synthetic accessibility of the series while optimizing the activity profile toward obtaining potent dual ACC1/2-inhibitors in both human and rodent. We tackled both goals by replacing the naphthyl ring of compound **3** with a phenyl ring and inserting an ethyl linker between ether oxygen and the cyclopentyl moiety, essentially clipping off part of the naphthyl ring as schematically indicated in Figure 2.

The resulting compound **4a** had a lower molecular weight than **3** and proved to be a dual ACC1/2 inhibitor, albeit weak on rat ACC. Because of its interesting in vitro profile, we decided to explore this scaffold further by systematically varying different parts of the molecule in subsequent SAR studies.

3.2. SAR Studies. Our structure−activity relationship (SAR) efforts focused initially on identifying whether either *m*- or *p*-substitution at the phenyl ring proved to be more promising (Tables 1, 4a−f). As could be seen from compounds **4a**−**d**, even small hydrophobic modifications in R2 with the *m*-substituted phenyl ring resulted in reduced ACC1/2 inhibition, indicating a steep SAR for this pattern and providing less synthetic options. We therefore focused on the *p*-substituted phenyl rings by introducing an oxygen atom in position X and shortening the chain length of the hydrophobic ether moiety in 4-position, denoted R3 (**4e**, **4f**). Compound **4e** cis/trans indicated that the stereochemical

Scheme 6[a]

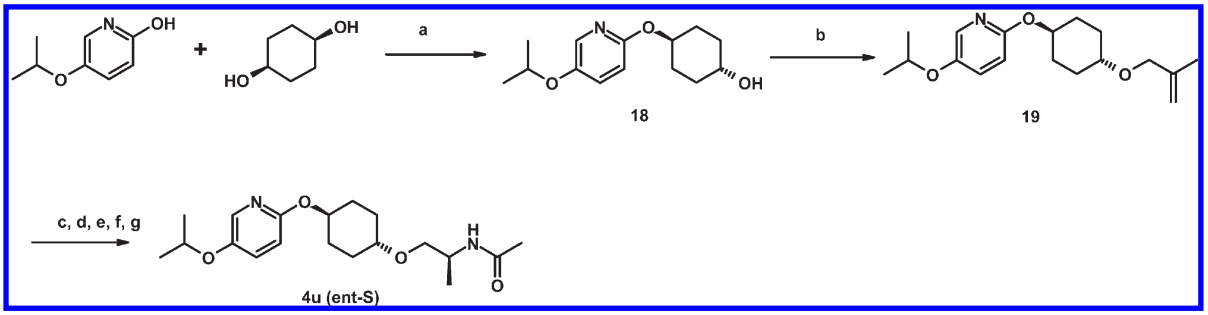

[a] Reagents and conditions: (a) PPh_3, DEAD, THF; (b) 3-bromo-2-methyl-propene, NaH, DMF; (c) OsO_4, $NaIO_4$, THF/H_2O, 0 °C; (d) BnNHOH then Pd/H_2; (e) $LiAlH_4$, THF; (f) Ac_2O, NEt_3, DCM; (g) HPLC on chiral phase

Scheme 7[a]

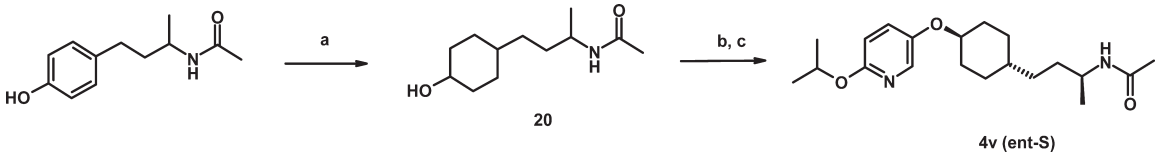

[a] Reagents and conditions: (a) 100 bar H_2, 5% Rh(C), 100 °C, ethanol; (b) isopropoxy-5-(4,4,5,5-tetramethyl-[1,3,2]dioxaborolan-2-yl)pyridine, $Cu(OAc)_2$, 1-butylimidazole, pyridine, toluene, 100 °C; (c) HPLC on chiral phase.

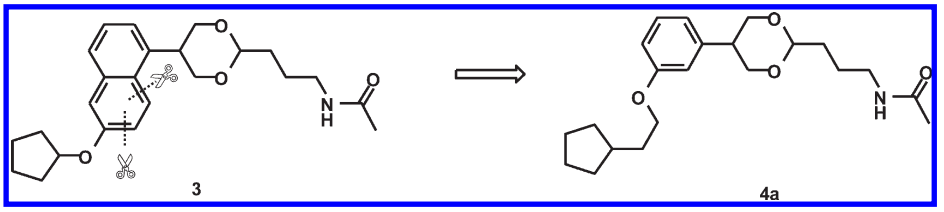

Figure 2. Chemical Optimization strategy of **3**.

requirements for ACC2 inhibition at the 1,3-dioxane moiety are *trans*-2,5-substitution.

Modulation of the electronic properties of the aromatic ring by replacing the phenyl group with a pyridine (**4g** versus **4e**-*trans*) proved to have a positive effect on hACC1/2 and rACC1 inhibition with no effect on rACC2.

In parallel to the 1,3-dioxane linker (position A) shown in Table 1, we also explored other linker groups, such as phenyl and cyclohexyl, for which we give examples in Table 2. These other linker moieties had the added bonus of enabling the easier introduction of a methyl (position R2 in Table 2) into the acetamide group, an effect that was described as beneficial for ACC inhibition by Gu et al[9] and that was verified by us (**4h** and **4i**). We also found that the (*S*)-enantiomer constitutes the more active compound[9] as can be seen from **4j**-(*S*) vs **4j**-(*R*) and **4m**-(*S*) vs **4m**-(*R*). Interestingly, whether the (*R*)-enantiomer retains weak activity on hACC1/2 (**4m**-(*R*)) or is inactive (**4j**-(*R*)) apparently depends on the size of the hydrophobic ether group in R3; for the smaller isopropyl group, more activity is retained.

Smaller hydrophobic ether groups in R3 seemed to be beneficial especially for the inhibition of rACC2 (**4j**, **4i**, **4l**) and resulted in a good overall ACC activity profile.

Since we learned from the SAR studies in the 1,3-dioxane part of the series that the replacement of the aromatic phenyl ring with a heterocycle could play an important role, we more fully evaluated such an effect by investigating different nitrogen containing six-membered heterocycles (**4j** and **4k**, **4l**−**4p**). It appeared that the exact position of the nitrogen was absolutely crucial, with nitrogen in position B leading to the most active compound **4m**-(*S*). The introduction of a second nitrogen atom (**4n**−**p**) drastically reduced activity on all tested ACC isoforms. Whether these effects were due to the modulation of properties of the aromatic ring to form $\pi-\pi$ interactions or whether this effect was due to a potential hydrogen-bonding capacity of the nitrogen atom in position B remains unclear on the basis of this data.

Modifications of R1 were also evaluated by us (**4q**−**4t**). A small hydrophobic group like methyl gives best activities (**4m**-(*S*)) while a cylcopropyl ring instead is well tolerated (**4s**). Hydrogen in R1 (**4q**) or the introduction of heteroatoms (**4r**, **4t**) apparently lead to the loss of hydrophobic interactions and thus reduced activity.

The sensitivity of the ACC isoform activity profile to small changes in the chemical structure (cf **4l**-(*S*) and **4m**-(*S*)) is also highlighted by the examples for the cyclohexyl linker **4u**-(*S*) and **4v**-(*S*). Compared with **4m**-(*S*), the exchange of the phenyl linker with cyclohexyl (**4v**-(*S*)) improved hACC2 and rACC2 by a factor of 2 while it simultaneously diminished rACC1 activity by a factor of 7 and hACC1 activity remained unchanged. The exchange of a methylene with an oxygen atom deteriorated the activity profile (**4u**-(*S*)) considerably.

In relation to the previously described inhibitors **1** and **2**, both **4m**-(*S*) and **4v**-(*S*) inhibited human ACC1/2 significantly more. **4m**-(*S*) was selected for further characterization because of its ease of synthesis and higher activity toward rat ACC1.

Table 1. Inhibitory Activities on Human and Rat ACC1 and ACC2[a]

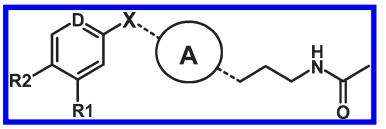

Cpd	R1	R2	A	D	X	Human IC50 [μM] ACC2	Human IC50 [μM] ACC1	Rat IC50 [μM] ACC2	Rat IC50 [μM] ACC1
4a	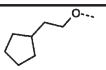	H		CH	bond	0.27	2.7	17	25
4b		H		CH	bond	2.65	>30	>30	>30
4c		H		CH	bond	2.1	>30	>30	>30
4d	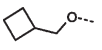	H		CH	bond	0.7	21	>30	>30
4e-cis	H	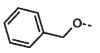		CH	O	>30	n.d	n.d	n.d.
4e-trans	H	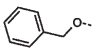		CH	O	0.4	>30	>30	>30
4f	H			CH	O	0.19	3.9	12	13
4g	H	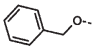		N	O	0.07	14.6	>30	14
1						0.06	>10	0.38	>10
2						0.07	0.91	0.28	0.59
3						0.63	>30	>30	>30

[a] The IC_{50} data are an average of at least three measurements.

3.3. Biological Characterization. 4m-(*S*) possessed no activity toward pyruvate carboxylase and PPARα, γ, and δ, respectively, and was inactive in a panel of 30 unrelated receptors, enzymes and transporters (data not shown). **4m**-(*S*) dose dependently increased fat oxidation in human liver cells, indicating cellular activity (Figure 3).

4m-(*S*) showed good plasma exposures after intravenous and oral administration (Tables 3 and 4) to female Wistar rats and a high bioavailability (F = 98%). The exposure in liver tissue after oral administration was high (Table 4, Figure 4). The liver/plasma ratios based on AUC_{0-inf} was calculated to be 6. Even 6 h after the oral dose of 10 mg/kg **4m**-(*S*), the concentration in liver tissue (approximately 5.5 μmol/kg) appeared to be still higher than that required to stimulate fat oxidation in liver cells (compare Figures 3 and 4). To characterize the activity of **4m**-(*S*) in vivo, we applied the compound at a dose of 50 mg/kg to rats followed by the administration of triglycerides and analyzed the respiration by indirect calorimetry. During the dark phase, RQ values of all groups became increased, as this is the animals' main feeding period (Figure 5). The lipid load resulted in a reduced RQ relative to the control group. **4m**-(*S*) decreased the RQ further, indicating a stimulation of fat oxidation by the drug in vivo. In relation to lean controls, obese female ZDF-rats have increased plasma triglyceride levels and are a model of dyslipidemia. Following the administration of **4m**-(*S*) for 3 days, plasma triglycerides decreased significantly in these animals compared to the treatment with vehicle only, indicating an improvement in dyslipidemia (Figure 6).

4. Conclusion

Overall we have identified in **4m**-(*S*) a compound with good in vitro activity toward human and rat ACC isoforms. The compound possessed favorable pharmacokinetic parameters, stimulated fat oxidation, and reduced plasma triglyceride levels after subchronic administration. This compound will be useful for further validation of ACC inhibition as a potential approach for the treatment of aspects of the metabolic syndrome.

5. Experimental Section

5.1. General Chemistry. Solvents and other reagents were used as received without further purification. Column chromatography

Table 2. Inhibitory Activities on Human and Rat ACC1 and ACC2[a]

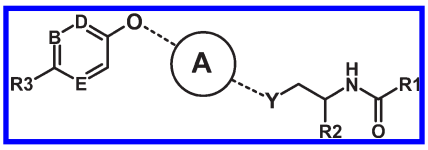

Cpd	R1	R2	R3	B	D	E	A	Y	Human IC50 [μM] ACC2	Human IC50 [μM] ACC1	Rat IC50 [μM] ACC2	Rat IC50 [μM] ACC1
4h	CH_3	H		CH	N	CH		CH_2	1.28	>30	>30	>30
4i	CH_3	CH_3		CH	N	CH		CH_2	0.14	1.1	7.9	2.9
4j	CH_3	CH_3		CH	N	CH		CH_2	0.21	0.75	>30	2.1
4j-(S)	CH_3	(S)-CH_3		CH	N	CH		CH_2	0.1	0.92	>30	1.2
4j-(R)	CH_3	(R)-CH_3		CH	N	CH		CH_2	>30	n.d	n.d.	n.d.
4k	CH_3	CH_3		N	CH	CH		CH_2	0.08	1.10	7.9	0.70
4l	CH_3	CH_3		CH	N	CH		CH_2	0.2	1.78	4.52	2.6
4l-(S)	CH_3	(S)-CH_3		CH	N	CH		CH_2	0.20	1.80	6.75	2.60
4m-(S)	CH_3	(S)-CH_3		N	CH	CH		CH_2	0.03	0.19	0.4	0.17
4m-(R)	CH_3	(R)-CH_3		N	CH	CH		CH_2	7.80	9.90	>30	>30
4n	CH_3	CH_3		N	CH	N		CH_2	0.7	3.0	20	7.4
4o	CH_3	CH_3		N	N	CH		CH_2	6.7	12.7	> 30	>30
4p	CH_3	CH_3		CH_2	N	N		CH_2	1.2	>30	>30	>30
4q	H	CH_3		N	CH	CH		CH_2	0.67	5.7	17	11
4r	OCH_3	CH_3		N	CH	CH		CH_2	0.25	1,2	3.9	2.9
4s		CH_3		N	CH	CH		CH_2	0.19	0.62	1.9	3.2
4s-(S)		(S)-CH_3		N	CH	CH		CH_2	0.08	0.36	0.7	0.8
4t	NH_2	CH_3		N	CH	CH		CH_2	0.15	1,2	3	2.9
4u-(S)	CH_3	(S)-CH_3		N	CH	CH		O	0.06	2.3	0.6	10.5
4v-(S)	CH_3	(S)-CH_3		N	CH	CH		CH_2	0.015	0.14	0.2	1.14

[a] The IC_{50} data are an average of at least three measurements. Enzyme potency variance was <25% for all compounds

was carried out on Merck silica gel 60 (230−400 mesh). Reversed phase high pressure chromatography was conducted on an Abimed Gilson instrument using a LiChrospher 100 RP-18e (5 μm) column from Merck. Thin-layer chromatography was carried

Table 3. Pharmacokinetic Parameters of **4m**(-*S*) in Plasma of Rats after Intravenous Dosing (3 mg/kg)

parameter[a]	plasma
C_{oh} (μmol/L)	5.2
$t_{1/2}$ (h)	1.5
$AUC_{(0-inf)}$ (μmol × h/L)	5.6
Cl (L/h/kg)	1.6
V_{dss} (L/kg)	2.6

[a] C_{oh}, **4 m**-(*S*) concentration immediately after dosing; $AUC_{(0-inf)}$, area under the curve; $t = 0$ until infinity; Cl, clearance; V_{dss}, volume of distribution at steady state

Table 4. Pharmacokinetic Parameters of **4m**(-*S*) in plasma and Liver of Rats after Oral Dosing (10 mg/kg)

parameter[a]	plasma	liver
C_{max} (μmol/L or/kg)	3.50	21.8
t_{max} (h)	2.0	2.0
C_{6h} (μmol/L or/kg)	1.59	7.59
$AUC_{(0-inf)}$ (μmol x h/l or/kg)	19	120
$t_{1/2}$ (h)	1.8	3.0

[a] C_{max}, maximal **4m**-(*S*) concentration; t_{max}, time of C_{max}; C_{6h}, concentration of **4 m**-(*S*) 6 h after oral administration; $AUC_{(0-inf)}$, area under the curve; $t = 0$ until infinity.

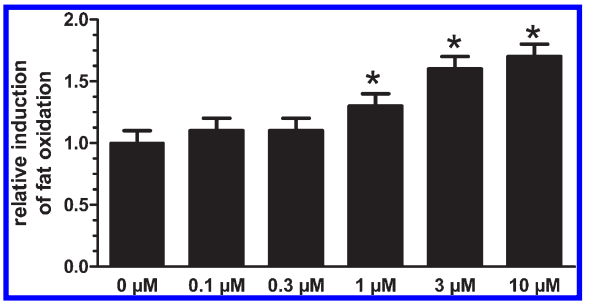

Figure 3. Stimulation of fat oxidation by **4m**-(*S*). Human hepatocytes were incubated in the presence of [^{3}H]palmitate and the indicated concentration of **4m**-(*S*). After 4 h, the release of ^3H_2O was measured. Results are expressed as the fold induction of fat oxidation in relation to controls (0 μM). Values are means ± SEM ($n = 4$) *$p < 0.05$ vs 0 μM **4m**-(*S*).

out on TLC aluminum sheets with silica gel 60F254 from Merck. Nuclear magnetic resonance (^{1}H NMR) spectra were recorded in DMSO-d_6 on a Bruker DRX 500 or in DMSO-d_6 or in $CDCl_3$ on an Avance II 400 or INCA 400. Chemical shifts are reported as δ values from an internal tetramethylsilane standard. HPLC-MS method A: Waters Aquity UPLC system was equipped with a Waters Aquity autosampler, UPLC pump and a diode array. The HPLC column used was a Waters Aquity BEH C-18 Column (2.1 mm × 50 mm, 1.7 μM) at a flow rate of 0.9 mL/min and at 55 °C. The HPLC eluent was coupled with a 1:3 split to a Waters Aquity SQD single quadrupole mass spectrometer with electrospray ionization. Spectra were scanned from 100 to 1300 amu in positive and negative mode. The eluents were A, water with 0.1% formic acid, and B, acetonitrile with 0.8% formic acid. Gradient elution from 5% B to 95%B over 1.1 min with a final hold at 95% B of 0.6 min. Total run time was 2 min. HPLC-MS method B: Agilent series 1100 system was equipped with a degasser G1322A, bin pump G1312A, ALS G1313A, col comp G1316A, DAD G1315A, and MSD G1946A. The HPLC column used was a YMC J sphere H80 (20 mm × 2 mm, 4 μM) at a flow rate of 1 mL/min. The HPLC eluent was coupled with a mass spectrometer with electrospray ionization. Spectra were scanned from 110 to 1000 amu in positive and negative mode. The eluents were A, water with 0.05% trifluoro acetic acid, and B, acetonitrile. Gradient elution from 4% B to 95%B over 2 min with a final

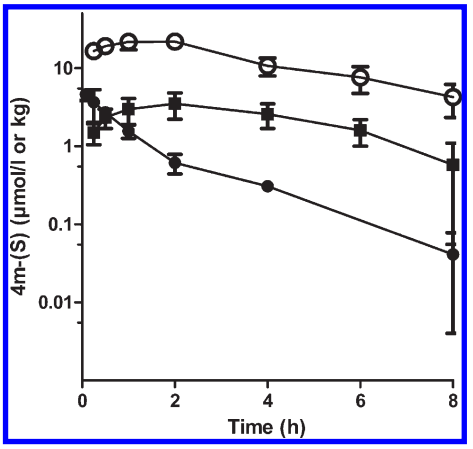

Figure 4. Pharmacokinetics of **4m**-(*S*) in rats. Plasma concentrations of **4 m**-(*S*) after 3 mg/kg iv administration (filled circles), plasma (filled boxes), and liver concentrations (open circles) after oral administration of 10 mg/kg **4m**-(*S*); values are means ± SD ($n = 3$).

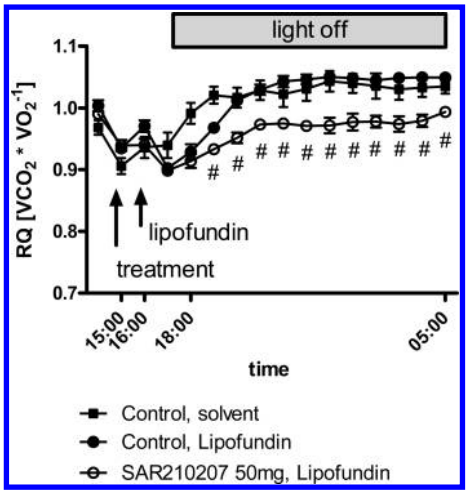

Figure 5. Lowering of RQ by **4m**-(*S*). Rats were administered either vehicle or **4m**-(*S*) (50 mg/kg), followed 2 h later by application of the lipid load. Arrows indicate time points of applications, vehicle group (filled boxes), lipid control group (filled circles), lipid/**4m**-(*S*) group (open circles). Values are means ± SEM ($n = 8$); *$p < 0.05$ vs vehicle group; # $p < 0.05$ vs lipid control group.

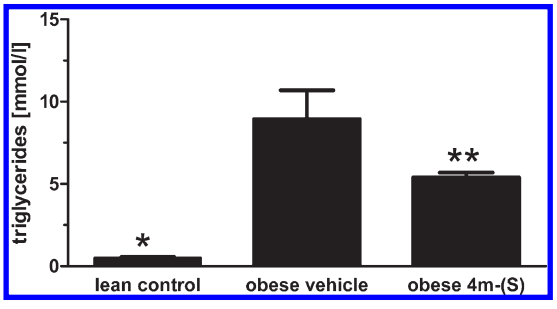

Figure 6. Reduction of plasma triglycerides in obese female ZDF rats by **4m**-(*S*). Plasma triglyceride levels in lean controls and female obese ZDF rats treated with either vehicle or 30 mg/kg **4m**-(*S*) for 3 days. Data are means ± SEM ($n = 8$), *$p < 0.05$ vs obese vehicle and obese **4m**-(*S*); **$p < 0.05$ vs obese vehicle.

hold at 95% B of 0.4 min. Total run time was 2.5 min. Purity and characterization of compounds were established by a combination of LC-MS and NMR analytical techniques. Generally, the purity of each compound is >95%. For selected compounds, the exact

purity is given in parentheses at the end of the description of its synthesis in the Experimental Section.

Reference compounds **1** (*N*-{(*S*)-3-[2-(4-isopropoxy-phenoxy)-thiazol-5-yl]-1-methyl-prop-2-ynyl}-acetamide) and **2** (anthracen-9-yl-[(*R*)-3-(morpholine-4-carbonyl)-[1,4′]bipiperidinyl-1′-yl]-methanone) were obtained using previously described synthetic procedures.

Procedure for the Synthesis of 4m. 5-(4-Bromo-phenoxy)-2-chloro-pyridine (12). First 39.0 g of 6-chloro-pyridin-3-ol and 177.5 g of 1,4-dibromo-benzene and were dissolved in 500 mL pyridine. Then 100 g of potassium carbonate and 85 g of freshly powdered CuO were added and the mixture was heated under reflux for 3 h. The mixture was cooled to 60 °C, 400 mL ethyl acetate were added, and the mixture was stirred for 20 min at 60 °C. Stirring was stopped and the mixture was filtered over a 350 g Celite pad. The solid was rinsed three times with 500 mL of hot ethyl acetate. The filtrate was concentrated in vacuo. The residual pyridine was removed by azeotropic distillation with 3 × 500 mL of toluene (1,4-dibromo benzene was codistilled or sublimated at low vacuum < 50 mbar). The black residue was suspended in 150 mL of toluene and filtered over 350 g of silica gel with *n*-heptane: ethyl acetate = 1:1. The solvent was removed in vacuo and the residue was purified by silica gel chromatography with the eluents *n*-heptane:ethyl acetate = 15:1 to obtain 38.9 g (45%) of **12**. ^{1}H NMR (500 MHz, DMSO-d_6) δ 8.27 (d, 1H), 7.64−7.52 (m, 4H), 7.08 (d, 2H). LC-MS: method B, R_t = 1.73 min (purity 100%); m/z 283.9, 285.9 ($M + H^+$).

5-(4-Bromo-phenoxy)-2-isopropoxy-pyridine (13). First, 13.67 g of sodium hydride (60% in mineral oil) were added in portions to 28 mL of isopropanol in 150 mL of *N*-methylpyrrolidon at room temperature with cooling (T > 25 °C). When the gas evolution had stopped (after about 1 h), 38.9 g of **12** dissolved in 20 mL *N*-methylpyrrolidon, was added via a dropping funnel and the mixture was heated to 85 °C for 3 h. After cooling to room temperature, 2 M HCl was added with cooling (pH 5), followed by 200 mL of saturated NH_4Cl solution. The mixture was extracted twice with 150 mL of *n*-heptane/ethyl acetate = 10:1. The combined organic layers were washed three times with 100 mL of half saturated NH_4Cl solution, 100 mL of brine, dried over $MgSO_4$, and then concentrated in vacuo. The residue was purified by silica gel chromatography with the eluent *n*-heptane: ethyl acetate = 60:1 to obtain 35.6 g (85%) of **13** as a yellowish oil. ^{1}H NMR (500 MHz, DMSO-d_6) δ 8.07 (d, 1H), 7.61−7.54 (m, 3H), 6.97 (d, 2H), 6.85 (d, 1H), 5.23 (m, 1H), 1.30 (d, 6H). LC-MS: method A, R_t = 1.41 min (purity 97%); m/z 308.0, 310.0 ($M + H^+$).

2-{(*S*)-3-[4-(6-Isopropoxy-pyridin-3-yloxy)-phenyl]-1-methyl-prop-2-ynyl}-isoindole-1,3-dione (14). First, 12.04 g of **13**, 11.7 g of (*S*)-2-(but-3-yn-2-yl)isoindole-1,3-dione, 372 mg copper-(I)iodide, and 16.3 mL of triethylamine were dissolved in 50 mL of dimethylformamide and degassed with argon for 20 min. Then 1.37 g of bis(triphenylphosphine)palladium(II) chloride were added and the reaction mixture was stirred at 70 °C for 5 h. The cooled reaction mixture was evaporated in vacuo, and the resulting residue was purified by silica gel chromatography with the eluent *n*-heptane:ethyl acetate = 1:1 to obtain 9.2 g (55%) of **14**. ^{1}H NMR (500 MHz, DMSO-d_6) δ 8.05 (d, 1H), 7.97−7.90 (m, 4H), 7.55 (dd, 1H), 7.43 (d, 2H), 6.94 (d, 2H), 6.82 (d, 1H), 5.38 (m, 1H), 5.21 (m, 1H), 1.72 (s, 3H), 1.30 (d, 6H). LC-MS: method B, R_t = 1.51 min, m/z 427.1 ($M + H^+$).

2-{(*S*)-3-[4-(6-Isopropoxy-pyridin-3-yloxy)-phenyl]-1-methyl-propyl}-isoindole-1,3-dione (15). First, 9.6 g of **14** were dissolved in 500 mL of ethanol and 200 mL of terahydrofuran. Then 4.80 g of palladium catalyst (10% palladium on charcoal) were added and the reaction mixture stirred at 3 bar hydrogen pressure for 3 h at room temperature. The reaction was then filtered through a Celite pad, the catalyst was rinsed three times with 300 mL of ethyl acetate, and then the filtrate was evaporated in vacuo to obtain 9.33 g (96%) of **15** as a yellow oil. ^{1}H NMR (500 MHz, DMSO-d_6) δ 7.93 (d, 1H), 7.88 (m, 3H), 7.37 (dd, 1H), 7.14 (d, 2H), 6.80 (d, 2H), 6.78 (s, 1H), 5.22 (m, 1H), 4.28 (m, 1H), 2.58 (m, 1H), 2.51 (m, 1H), 2.35 (m, 1H), 1.99 (m, 1H), 1.40 (d, 3H), 1.28 (d, 6H). LC-MS: method B, R_t = 1.26 min, m/z 431.2 ($M + H^+$).

(*S*)-3-[4-(6-Isopropoxy-pyridin-3-yloxy)-phenyl]-1-methyl-propylamine (16). First, 10.3 g of **15** were dissolved in 400 mL of ethanol and 10 mL of hydrazine hydrate were added. Then the reaction mixture was heated under reflux for two hours. The cooled mixture was filtered through a Celite pad and the filtrate washed with saturated $NaHCO_3$ solution and brine and dried over $MgSO_4$, and then the solvent was removed in vacuo to obtain 7.28 g of **16**. ^{1}H NMR (500 MHz, DMSO-d_6) δ 8.03 (d, 1H), 7.52 (dd, 1H), 7.26 (d, 2H), 6.95 (d, 2H), 6.84 (d, 2H), 5.24 (m, 1H), 2.79 (m, 1H), 2.60 (m, 2H), 1.52 (m, 2H), 1.29 (d, 6H), 0.99 (d, 3H). LC-MS: method B, R_t = 0.74 min, m/z 301.2 ($M + H^+$).

***N*-{(*S*)-3-[4-(6-Isopropoxy-pyridin-3-yloxy)-phenyl]-1-methyl-propyl}-acetamide (4m(ent-*S*)).** First, 1.96 g of **16** was dissolved in 150 mL of ethyl acetate and 2.0 mL of triethylamine were added. Upon cooling in an ice bath, 0.44 mL of acetic acid anhydride were added. The ice bath was removed and the reaction mixture stirred at room temperature for 3 h. Then the reaction mixture was concentrated under reduced pressure and the resulting residue taken up in water/ethyl acetate. The water phase was separated and extracted five times with ethyl acetate. The combined organic layers were dried over $MgSO_4$, the solvent removed in vacuo, and the residue purified by reverse phase HPLC to obtain 1.56 g (97%) of **4m**(ent-*S*). ^{1}H NMR (500 MHz, DMSO-d_6) δ 8.03 (d, 1H), 7.80 (d, 1H), 7.52 (dd, 1H), 7.24 (d, 2H), 6.94 (d, 2H), 6.84 (d, 1H), 5.25 (m, 1H), 3.76 (m, 1H), 2.54 (m, 2H), 1.81 (s, 3H), 1.62 (m, 2H), 1.29 (d, 6H), 1.03 (d, 3H). LC-MS: method A, R_t = 1.68 min (purity 100%), m/z 343.2 ($M + H^+$); enantiomeric purity 99.7%, R_t = 6.569 min, stationary phase Chiralcel OJ-H/62 250 mm × 4.6 mm, eluent *n*-heptane:ethanol: methanol = 10:1:1.

Using racemic 2-(but-3-yn-2-yl)isoindole-1,3-dione and following the procedure as in the preparation of **4m**(ent-*S*) gave racemic **4m**. The racemic mixture of **4m** was separated on chiral phase (Chiracel OJ/H58, *n*-heptane:ethanol:methanol = 10:1:1) to give **4m**(ent-*S*) (enantiomeric purity 100%, R_t = 6.599 min) and **4**(ent-*R*) (enantiomeric purity 100%, R_t = 5.211 min)

5.2. Biology. In Vitro Assays. Protein Production. Recombinant ACC enzymes were expressed in baculovirus-infected High Five insect cells as N-terminal His-tagged fusion proteins and purified by Ni-affinity and size exclusion chromatography. The human ACC1 and ACC2 proteins consisted of the amino acids 2-2346 and 27-2458, respectively, rat ACC1 and ACC2 included amino acids 1-2345 and 27-2455, respectively. Bovine pyruvate carboxylase was obtained from Sigma.

Enzymatic and Cellular Assays. ACC enzymatic activity was determined via an ATP consumption assay. The assays were performed in 96-well plates and included 50 mM Tris-acetate, 16 mM $NaHCO_3$, 0.9 mg/mL BSA, 25 μM ATP, 1.14 μM β-mercaptoethanol, 4.3 mM magnesium acetate, 0.25 mM acetyl CoA, 1% DMSO, and 200 ng of enzyme per well. The ACC inhibitor was added at concentrations between 0 and 10 μM. The reaction was started by the addition of enzyme (200 ng/well) followed by incubation for 90 min at 37 °C. Unconverted ATP was determined using the ATP monitoring reagent (Cambrex, Charles City, USA) according to the manufacturer's instructions. IC_{50} was calculated as the inhibitor concentration that reduced the ATP turnover by 50% relative to a sample without inhibitor.

The rate of cellular ss-oxidation of [9,10(n)-^{3}H]palmitic acid was measured as ^3H_2O release.[14] HepG2 were seeded in 24-well dishes (200000 cells/well). After attachment, the cells were washed once with PBS and subsequently incubated in the presence of DMEM, 5 μM (15000 Bq/ml) ^{3}H-palmitic acid, 0.2 mg/mL BSA, 500 μM L-carnitine, 0.1 (v/v) % DMSO in the presence of glucose (25 mM) and the ACC inhibitor. β-oxidation was initiated by the addition of 0.5 μCi [^{3}H]palmitate to the incubation medium.

After 4 h at 37 °C, portions of the cell supernatants were loaded onto Sep-Pak cartridges (Waters, Eschborn, Germany). Unbound radioactivity was measured by liquid scintillation counting.

5.3. In Vivo Experiments. Pharmacokinetic Studies. Pharmacokinetic parameters of **4m**-(*S*) were determined in Wistar rats (Harlan Winkelmann, Paderborn, Germany). After intravenous bolus administration of 3 mg/kg of **4m**-(*S*) in 5% solutol solution, plasma samples were taken at eight time points over 24 h. After a single oral administration of 10 mg/kg of **4m**-(*S*) in 10% DMSO, plasma and tissue samples were taken at eight different time points over 24 h. Three animals were killed at each time point. The respective concentrations of **4m**-(*S*) in plasma and tissues were determined by LC-MS/MS. Quantification was performed with help of an internal standard.

Indirect Calorimetry. The setting consisted of 17 cages, of which 16 were used for individual housing of the animals during the study, and one cage served as the reference cage for corrections of O_2 and CO_2 measurements. Female Wistar rats were accustomed to the cages at least 12 h before the start of the measurements (day −1). O_2 consumption and CO_2 production were measured every 17 min/cage for 1 min (gas analyzers: Magnos 16 and Uras 14; ABB, Frankfurt/Main, Germany) and recorded on a computer. Animals were treated orally with either 50 mg/kg of **4m**-(*S*) or vehicle. Two hours later, animals were given orally either 10 mL/kg of 20% Lipofundin MCT (B. Braun, Melsungen, Germany) corresponding to 2 g fat/kg or vehicle (PBS). Values are expressed as the means of liters per hour. RQ was calculated as the quotient of CO_2 production/O_2 consumption, with the value of 1 representing 100% carbohydrate oxidation and the value of 0.7 representing 100% fat oxidation.[15]

In Vivo Pharmacology. Female lean (Fa/?) and obese (fa/fa) ZDF rats [ZDF-Lepr^{fa}/Crl] (Charles River (Sulzfeld, Germany) were maintained two per cage on a constant 12-h light/dark cycle (light on 06:00) under controlled temperature and humidity conditions. Water was freely accessible. They were fed with SSNIFF pellet chow (Soest, Germany) ad libitum. At the age of eight weeks, eight rats were treated orally for three days with 30 mg/kg **4m**-(*S*) dissolved in 5% ethanol, 5% solutol, 90% PBS; the control rats received the vehicle alone. Four hours after the last administration, rats were euthanized in deep isoflurane anesthesia and blood was collected from the aorta after laparotomy for determination of triglycerides on a Hitachi 912 using the GPD-PAP kit (Roche, Mannheim, Germany).

Acknowledgment. We gratefully acknowledge the technical assistance of Gerhard Burdinski, Silvia Fischer, Katrin Kern, Marion Meyer, Anke Müller-Seeland, Jan Oehme, Sascha Rauch, and Hermut Albrecht Wehlan. We thank Dr. Carolyn Schmoll for critical reading of the manuscript.

Supporting Information Available: Experimental and spectroscopic data of test compounds **4a**−**4l**, **4n**−**4v** and of intermediate compounds **5**−**9**, **10e**, **10g**, **18**−**20**. This material is available free of charge via the Internet at http://pubs.acs.org.

References

(1) Dargazanli, G.; Lardenois, P.; Frost, J.; George, P. Preparation of *N*-[(naphthyldioxanyl) propyl]glycinates and analogs as neuroprotectants. (*Synthelabo SA, France*). Patent WO9855474 A1 1998.
(2) Zoller, G.; Schmoll, D.; Mueller, M.; Haschke, G.; Focken, I. Heterocyclic compounds, processes for their preparation, medicaments comprising these compounds, and the use thereof. Patent WO2010003624 A2, 2010.
(3) Shibata, M.; Kihara, Y.; Taguchi, M.; Tashiro, M.; Otsuki, M. Nonalcoholic fatty liver disease is a risk factor for type 2 diabetes in middle-aged Japanese men. *Diabetes Care* **2007**, *30*, 2940–2944.
(4) Stefan, N.; Kantartzis, K.; Häring, H. U. Causes and metabolic consequences of Fatty Liver. *Endocr. Rev.* **2008**, *29*, 939–960.
(5) Harwood, H. J., Jr.; Petras, S. F.; Shelly, L. D.; Zaccaro, L. M.; Perry, D. A.; Makowski, M. R.; Hargrove, D. M.; Martin, K. A.; Tracey, W. R.; Chapman, J. G.; Magee, W. P.; Dalvie, D. K.; Soliman, V. F.; Martin, W. H.; Mularski, C. J.; Eisenbeis, S. A. Isozyme-nonselective *N*-substituted bipiperidylcarboxamide acetyl-CoA carboxylase inhibitors reduce tissue malonyl-CoA concentrations, inhibit fatty acid synthesis, and increase fatty acid oxidation in cultured cells and in experimental animals. *J. Biol. Chem.* **2003**, *278*, 37099–37111.
(6) Wakil, S. J.; Abu-Elheiga, L. A. Fatty acid metabolism: target for metabolic syndrome. *J. Lipid Res.* **2009**, *50* (Suppl), S138–S143.
(7) Corbett, J. W. Review of recent acetyl-CoA carboxylase inhibitor patents: mid-2007−2008. *Expert. Opin. Ther. Pat.* **2009**, *19*, 943–956.
(8) Beutel, B. A.; Camp, H. S.; Clark, R. F.; Gu, Y.-G.; Hansen, T. M.; Keyes, R. F.; Li, Q.; Liu, G.; Sham, H. L.; Wang, X.; Weitzberg, M.; Xin, Z.; Xu, X.; Zhang, T. Preparation of novel acetyl-CoA carboxylase (ACC) inhibitors and their use in diabetes, obesity and metabolic syndrome. US Patent US 2006178400 A1, 2006.
(9) Gu, Y. G.; Weitzberg, M.; Clark, R. F.; Xu, X.; Li, Q.; Zhang, T.; Hansen, T. M.; Liu, G.; Xin, Z.; Wang, X.; Wang, R.; McNally, T.; Camp, H.; Beutel, B. A.; Sham, H. L. Synthesis and Structure−Activity Relationships of *N*-{3-[2-(4-Alkoxyphenoxy)thiazol-5-yl]-1-methylprop-2-ynyl}carboxy Derivatives as Selective Acetyl-CoA Carboxylase 2 Inhibitors. *J. Med. Chem.* **2006**, *49* (13), 3770–3773.
(10) Gu, Y. G.; Clark, R. F.; Li, Q.; Weitzberg, M.; Sham, H. Novel Acetyl-CoA Carboxylase (ACC) Inhibitors and their use in diabetes, obesity and metabolic syndrome. Patent WO2008079610, 2008.
(11) Perry, D. A.; Harwood, H. J., Jr. Preparation of bipiperidinyl and related compounds as acetyl CoA carboxylase inhibitors useful against metabolic syndrome and other disorders. Patent WO 2003072197 A1, 2003.
(12) Savage, D. B.; Choi, C. S.; Samuel, V. T.; Liu, Z. X.; Zhang, D.; Wang, A.; Zhang, X. M.; Cline, G. W.; Yu, X. X.; Geisler, J. G.; Bhanot, S.; Monia, B. P.; Shulman, G. I. Reversal of diet-induced hepatic steatosis and hepatic insulin resistance by antisense oligonucleotide inhibitors of acetyl-CoA carboxylases 1 and 2. *J. Clin. Invest.* **2006**, *116*, 817–824.
(13) Tong, L.; Harwood, H. J., Jr. Acetyl-Coenzmye A Carboxylases: Versatile Targets for Drug Discovery. *J. Cell. Biochem.* **2006**, *99*, 1476–1488.
(14) Minnich, A.; Tian, N.; Byan, L.; Bilder, G. A potent PPARα agonist stimulates mitochondrial fatty acid beta-oxidation in liver and skeletal muscle. *Am. J. Physiol. Endocrinol. Metab.* **2001**, *280*, E270–E279.
(15) Herling, A. W.; Kilp, S.; Elvert, R.; Haschke, G.; Kramer, W. Increased energy expenditure contributes more to the body weight-reducing effect of rimonabant than reduced food intake in candy-fed wistar rats. *Endocrinology* **2008**, *149*, 2557–2566.